Volume Title
ASP Conference Series, Vol. **Volume Number**
Author

The CALIFA survey: Calibration plan

B. Husemann[1], S. F. Sánchez[2], and J. Falcón-Barroso[3,4], and D. Mast[2], and R. García-Benito[2], and the whole CALIFA collaboration

[1] *Leibniz-Institut für Astrophysik, An der Sternwarte 16, D-14482 Potsdam, Germany*

[2] *Instituto de Astrofísica de Andalucia (CSIC), Camino Bajo de Huetor, s/n, 18008, Granda, Spain*

[3] *Instituto de Astrofísica de Canarias, Vía Láctea s/n, La Laguna, Tenerife, Spain*

[4] *Departamento de Astrofísica, Universidad de La Laguna, E-38205 La Laguna, Tenerife, Spain*

Abstract. The currently ongoing Calar Alto Legacy Integral Field Area (CALIFA) survey is aimed to observe ~600 galaxies in the local Universe ($0.005 < z < 0.03$). It is the largest survey to date using optical integral field spectroscopy. Here, we shortly introduce the main characteristics of the survey and discuss a few important steps related to the calibration of the data, focussing on the spectrophotometry and astrometry. Error estimation is always needed for a proper interpretation of astronomical data, so CALIFA will provide proper errors associated with the data. However, all CALIFA users need to be aware of the correlated noise that is unavoidable present in the data as we highlight at the end. We find that the overall quality of the data is excellent for all the core CALIFA science goals, but we are already prepared to increase the accuracy even more for future data releases.

1. Introduction

Large imaging and spectroscopic surveys such as the 2dFGRS (Folkes et al. 1999), SDSS (York et al. 2000), GEMS (Rix et al. 2004), VVDS (Le Fèvre et al. 2004), and COSMOS (Scoville et al. 2007) have substantially increased our understanding of the Universe across cosmic times. For the first time it was possible to study integrated galaxy properties like luminosity, stellar mass, star formation rate, metallicity, etc., for a large sample of galaxies. The large sample size has been crucial to perform comparison studies for certain subsets of galaxies, which covered a broad range of galaxy types, as well as to study the effect of different environments.

Despite the tremendous success of these surveys, their information content is still limited in an astrophysical sense. Imaging surveys provide spatially resolved light distribution of galaxies, but with an extremely low spectral resolution of the spectral energy distribution (SED) due to large width of the broad band filters used. The next generation medium-band photometric surveys like COMBO-17 (Wolf et al. 2003), ALHAMBRA (Moles et al. 2008), COSMOS (Scoville et al. 2007) significantly improved

the sampling of the SED for better redshift and stellar mass estimates. However, they are still not able to resolve any absorption or emission line in the galaxy SED, which offer important insights into the evolution of galaxy properties. On the other hand, large spectroscopic surveys like SDSS (York et al. 2000) or VVDS (Le Fèvre et al. 2004) recorded optical spectra for a large number of galaxies, but these do not contain any spatially resolved information. This leads to significant aperture biases which are difficult to control.

To circumvent these problems, integral field spectroscopy (IFS) combines the advantages of imaging and spectroscopy albeit with a typically small field of view (a few tens of arcseconds). The technique of IFS has only been used for small surveys with a focussed science goal so far. Some examples are the SAURON/ATLAS3D survey targeting at 260 early-type galaxies at $z < 0.01$ (Cappellari et al. 2011), the PINGs project (Rosales-Ortega et al. 2010) to spatially map HII regions in very nearby disc galaxies ($\lesssim$10 Mpc) and a survey of 70 (ultra) luminous infrared galaxies at $z < 0.26$ using various IFS instruments.

The Calar Alto Legacy Integral Field Area (CALIFA) survey, currently being carried out at the Calar Alto observatory, will target 600 representative galaxies in the nearby Universe ($0.005 \leq z \leq 0.03$) with the technique of IFS for which 210 dark nights have been granted. An international collaboration of more than 80 scientist across 13 countries, which are lead by the PI S.F. Sánchez, is currently exploiting the data to address several open key questions in the evolution of galaxies: (1) What is relative importance of minor and major merging?; (2) What role play internal dynamical processes, such as bar, spiral arms, or stellar migration?; (3) How does the environment affect the galaxy properties?; (4) How does stellar and AGN feedback shape the properties of galaxies?; (5) What is the star formation history of galaxies? Additionally, the fully reduced data obtained by CALIFA will be made public to the astronomical community. This will allow much broader range of scientific exploitation and serendipitous discoveries, which represents and extraordinary legacy value of CALIFA in the near future.

2. Sample selection and observing strategy

A well-defined sample of galaxies has been selected from the SDSS DR7 photometric catalogue taking into account the scientific aims of the survey, technical constraints, and observational boundary conditions. A detailed description of the sample selection is presented in Sánchez et al. (2012) and Walcher et al. (in prep.), so that we only briefly describe it here. The main selection criteria for the sample are an apparent SDSS *r*-band isophotal diameter of $45'' < D_{25} < 80''$ to efficiently use the instrument field of view (FoV) and a redshift range of $0.005 < z < 0.03$ to allow for a fixed spectral setup as well as to limit the number of faint dwarf galaxies. Unfortunately, the spectroscopic galaxy catalogue of SDSS becomes increasingly incomplete at $r < 14$ mag, so that not all galaxies with a matching diameter have an assigned SDSS redshift. This gap in information is filled by complementing the redshift information with the data accessible through the SIMBAD database at CDS. Additionally, only galaxies with $\delta > 7^\circ$ have been selected in the North Galactic hemisphere of SDSS to ensure a good visibility from Calar Alto observatory, while no restriction was made for galaxies at southern Galactic latitudes to compensate for the smaller SDSS footprint in this area on the sky.

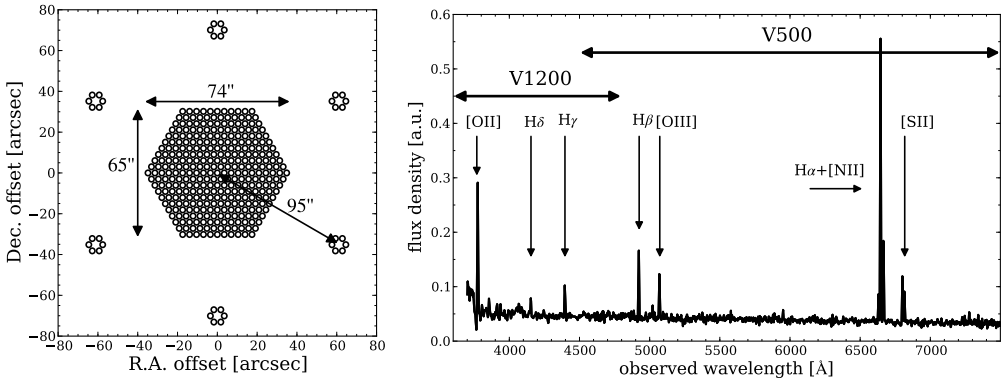

Figure 1. Instrumental characteristics of the PMAS-PPAK instrument as used for the CALIFA survey. *Left panel:* Relative position of the PPAK fibers on the sky. The central hexagonal field of view consists of 331 fiber, which are complemented with 36 sky fibers at a distance of $\sim 95''$ around the center of the hexagon. *Right panel:* Unvignetted wavelength range covered by the V500 and the V1200 grating setup of CALIFA, respectively. The underlying spectrum correspond to a typical galaxy spectrum and the strong emission lines are labelled.

With these rather small set of selection criteria, we obtained a sample of 939 galaxies in the local universe which is referred to as the "CALIFA mother sample".

From the CALIFA mother sample described above, 600 galaxies will be randomly selected for observation based on their visibility on the sky. The observations are performed with the Potsdam Multi Aperture Spectrograph (PMAS, Roth et al. 2005) using the PPAK fiber bundle, which consists of 382 fibers with a size of $2.7''$ in diameter on the sky. In Fig. 1 (left panel) we show the covered area of each fiber as projected on the sky. The primary science field consists of a large hexagonal bundle of 331 fibers with a $74'' \times 64''$ FoV and a filling factor of ∼2/3. To aid the simultaneous estimation of the sky background, 36 fibers are distributed in bundles of 6 fibers along a circle with a radius of $95''$ around the centre of the hexagonal FoV. The remaining 15 fibers are for calibration purposes only and are connected to the internal lamps of the instrument.

The PMAS instrument was upgraded in 2009 with an E2V CCD231 4k×4k chip that nominally increased the covered wavelength range. However, the four corners of the CCD became strongly affected by vignetting so that 25% of the wavelength range is lost for fibers near the edges of the CCD. Each galaxy is observed in two different and complementary setups to compensate for this effect while increasing the scientific value of CALIFA at the same time. The first setup uses a V500 grating with a nominal resolution of $R \sim 850$ at 5000Å and wavelength range of 3745–7300Å (4200–6850Å unvignetted). The V1200 grating is used for the second setup and provides a nominal resolution of $R \sim 1650$ at 4500Å and wavelength coverage of 3400–4750Å (3600–4550Å unvignetted). The broader wavelength coverage of the V500 setup is targeted for stellar population studies as well as to characterize the ionised gas from several emission lines. On the other hand, the higher resolution V1200 setup is ideal to obtain the stellar and ionised gas kinematics from the strong H+K stellar absorption lines and the [O II]$\lambda\lambda 3726, 3729$ emission line, respectively.

Three dithered pointings are taken in each setup to compensate for the inhomogeneous spatial coverage of a single pointing and to reach a filling factor of 100% across

almost the entire FoV. The exposure times were chosen based on extensive experience with the instrument to observe nearby galaxies (Sánchez et al. 2007; Rosales-Ortega et al. 2010; Mármol-Queraltó et al. 2011; Viironen et al. 2012). A single exposure of 900 s is taken for each pointing in the V500 setup and 2 subsequent 900 s exposures are acquired for each pointing in the V1200 setup to reach an almost similar depth compared to the V500 setup.

3. Calibration plan and future improvements

The variety of science drivers for the CALIFA survey also demands a certain calibration accuracy in many aspects. Kinematical studies of galaxies rely on the accuracy of the wavelength calibration and a characterisation of its uncertainty across the FoV. Studies interested in the stellar population of galaxies will compare the observed spectra with synthetic ones to infer the star formation history. They also require a homogeneous wavelength calibration to match the spectra, but more importantly a good relative flux calibration across the covered wavelength range from the blue to the red end of the all the spectra. Given that CALIFA obtains spectra across the entire galaxy allows to determine integrated quantities of the galaxies, such as stellar masses or star formation rates, which demands an absolute flux calibration to properly convert from apparent fluxes to luminosities. A high astrometric calibration of the CALIFA data seem to be not necessary at first glance. However, multi-wavelength ancillary data in the X-ray, UV, IR, and radio regime are available which need to be properly aligned to the CALIFA data for a proper scientific analysis. Additionally, the image reconstruction as explained below is only accurate when the relative positions of the individual pointings are accurately known.

3.1. General data reduction scheme

The complexity of IFS data and the diversity in the characteristics of the corresponding instruments is a huge problem for the data reduction. IFS data reduction can still be considered as an art, for which extensive experience with the instrument and IFS data is necessary. A dedicated data reduction pipeline was specifically designed for the CALIFA survey that runs autonomous usually without any manual intervention. Initially, the pipeline was based on R3D (Sánchez 2006) coded in Perl and C, but it is currently being upgraded and migrated to a newly developed IFS reduction platform based purely on Python called “Py3D”. The main reason for the transition is to take advantage of the growing Python community in astronomy and to simplify the maintenance of the pipeline along the duration of the survey and even beyond.

The pipeline reduces the data right after the observations of each night were finished. The raw data are processed already to science grade data in one pass, while taking into account several instrument and atmospheric characteristics, such as bias subtraction, cosmic ray detection, instrumental focus, instrument flexure, flat-fielding, wavelength calibration, sky subtraction, flux calibration, image reconstruction, differential atmospheric refraction correction, etc. All these steps are outlined in Sánchez et al. (2012) in more detail. In the following we just highlight a few challenging aspects of the CALIFA data calibration, evaluate their performance and present ideas to improve quality even further.

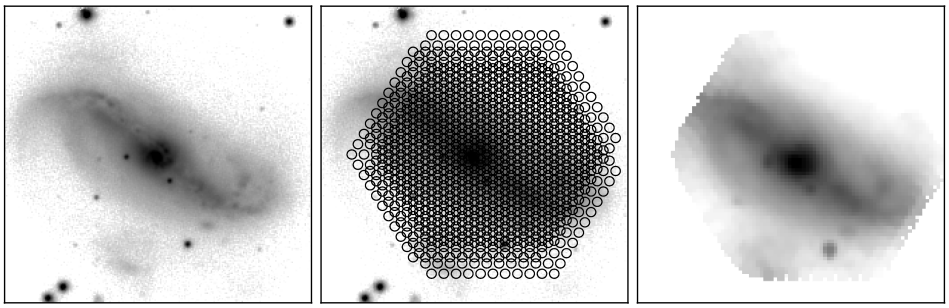

Figure 2. Example for the image reconstruction process for the CALIFA data. *Left panel:* SDSS *r* band image of a galaxy within the CALIFA sample. *Middle panel:* Overlaid position of each fiber of the three dither pointings. Most of the covered field is fully covered by at least one fiber. *Right panel:* Reconstructed image from the flux in the fibers using the distance-weighting algorithm as described in the text. The spatial resolution of the SDSS image cannot be achieved because of the relatively large fiber diameter of 3″.

3.2. Image reconstruction and astrometric calibration

In order to homogeneously cover the hexagonal PPAK FoV one need to cover the gaps between the fibers. This is solved with a three pointing dither scheme, which is shown in Fig. 2. The full coverage allows to reconstruct an image with a regular grid of pixels for each wavelength applying a dedicated resampling scheme, which produces a three-dimensional cube at the end. We used a simple inverse-distant weighting scheme as described in Sánchez et al. (2012), where the flux in each spatial pixel F_{ij} of the final reconstructed image can be computed from the original fiber flux f_k as

$$F_{ij} = \sum_{k=1}^{k=n} w_{ij}^k f_k \qquad . \tag{1}$$

The weights w_{ij}^k follow a Gaussian distribution according to the distance r_{ij}^k of the fiber k with the corresponding pixel (i, j) in the image plane:

$$w_{ij}^k = N \exp(-0.5(r_{ij}^k)^2) \tag{2}$$

where N is the normalization factor such that $\sum_{k=1}^{k=n} w_{ij}^k N = 1$. The reconstructed image of one example galaxy is shown in Fig. 2. We choose a final pixel size of 1″ compared to an initial fiber diameter of 2.7″. Although it is clear that reconstructed image is intrinsically undersampled with respect to the fiber diameter, the 1″ grid size has the advantage that absolute fluxes and surface brightnesses can be easily converted to each other.

An accurate knowledge of the initial position of each fiber is crucial to properly reconstruct the final CALIFA datacubes. The offsets of the dither pointings are fixed for all CALIFA observations and we currently rely on this a-priori knowledge to assign the position of each fiber relative to the others. Furthermore, we empirically determine the peak of the light distribution in the reconstructed image of the galaxy to assign the known reference coordinate of the galaxy to this pixel. However, a few galaxies do

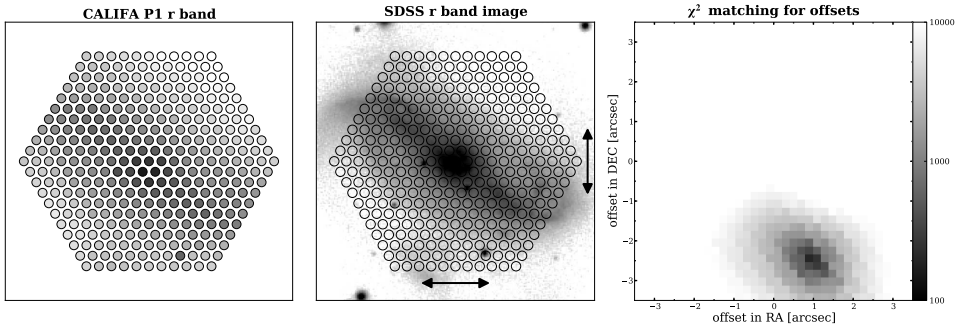

Figure 3. Visualization of the image registration technique for CALIFA currently being tested. *Left panel:* Synthesized broad-band flux distribution for the individual fibers of one single PPAK pointing. *Middle panel:* The fiber coverage is overlaid on a corresponding SDSS broad-band image with an arbitrary position with respect to the galaxy center. This relative position can be varied before the aperture flux of each fiber is extracted from the SDSS image. *Right panel:* χ^2 value of the CALIFA and SDSS flux comparison for a regular grid of offsets in right ascension and declination. The best matching fiber positions with respect to the galaxy center in the SDSS image is very well defined and the exact position of PPAK on the sky can be estimated with subarcsec precision.

not have a well-defined galaxy center and pointings offsets can be subject to human errors when manually entering the offsets to the telescope control system. In order to automatically handle these cases, we investigated the possibility to infer the relative position of each pointing individually to subarcsecond precision by registering each pointing on the reference SDSS image.

The steps of this process are outline in Fig. 3. First we extract synthetic broad-band fluxes from the spectra of each fiber together with its associated uncertainty. Second, we extract the brightness in fluxes within 2.7″ apertures at the assumed position of each fiber from the SDSS broad-band image for which we take into account the fractional pixel coverage of each fiber. The goodness of the match can be estimated by the χ^2 statistics:

$$\chi^2 = \sum_k \frac{\left(f_k^{\mathrm{CALIFA}} - f_k^{\mathrm{SDSS}}\right)^2}{\left(\sigma_k^{\mathrm{CALIFA}}\right)^2 + \left(\sigma_k^{\mathrm{SDSS}}\right)^2} \tag{3}$$

With a brute-force approach the χ^2 value can be computed for different pointing positions varied along the right ascension and declination. We find that the minimum in χ^2 is very well defined and allows to pin-point the position of the individual PPAK pointing on the sky relative to the SDSS image with sub-arcsecond precision. With this technique the uncertainty in the position of the PPAK pointing is not limited by the fiber size any more, but rather by the size of the SDSS image pixels. Whether the mismatch in the seeing of the CALIFA and the SDSS observations makes a strong difference in the cross-match is currently unclear and requires further tests. We therefore did not implemented this scheme in the current version of the data reduction pipeline so far and leave this for the next version.

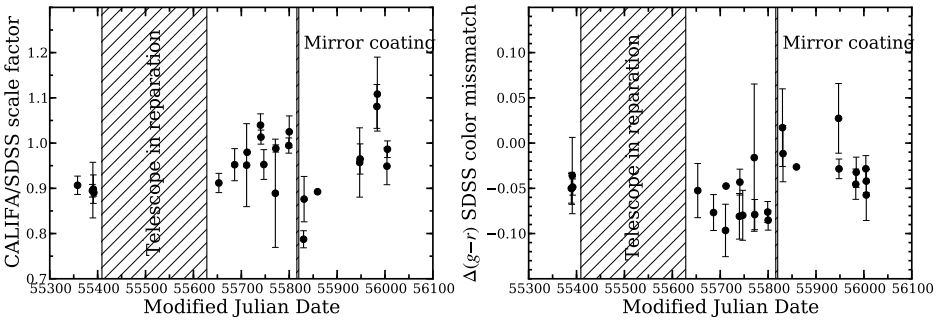

Figure 4. Evolution of the intrinsic spectrophotometric calibration with time along the duration of the survey so far. *Left panel:* Ratio between the integrated flux within a 30″ aperture of the reconstructed CALIFA and the SDSS *r* band image as a function of time. This factor is used to anchor the absolute photometry of the CALIFA data to the SDSS photometry. *Right panel:* Color offset between the CALIFA and SDSS $g - r$ magnitudes as a function of time. A period in time where the telescope was being repaired is indicated by the shaded area and the time of the mirror re-coating is indicated by the vertical line.

3.3. Absolute and relative photometric calibration

Standard star observations are part of the calibration data taken for the CALIFA survey at the beginning and end of each night if the weather permits. Standard stars are not observed for a significant fraction of nights, so that we currently used an *average* sensitivity function for consistency. This *average* sensitivity function was derived as the average of the ones obtained in two truly photometric nights. Anyway, the transparency of the atmosphere can significantly change during nights. The standard star observations therefore only provide a relative spectrophotometry along the wavelength which should be stable with time, but an absolute photometric recalibration is unavoidable. Because the CALIFA sample is drawn from the SDSS, we can anchor the CALIFA photometry to the calibrated broad-band SDSS images. The spectral range of the CALIFA V500 setup fully covers the *g* and *r* bands, so that synthetic broad-band images can be directly extracted from the datacubes. The flux within a 30“ aperture around the galaxy centre is obtained for CALIFA and SDSS in both band, so that any mismatch in the absolute photometric calibration can be quantified and corrected.

In Fig. 4 we show the photometric re-scaling factor against observing time for all observations in the V500 setup till February 2012. We find that the intrinsic absolute photometry of the fixed calibration varies by more than 30% as expected, but the spread for a certain night can be as low as a ±2% for photometric nights. The strong variation of the intrinsic photometry with time is not random, but rather follow a certain pattern. The sudden change in the intrinsic photometry by about 25% coincides exactly with the time at which the mirror was re-coated. This shows that the intrinsic photometric calibration, while using an *average* sensitivity function, is mainly modulated by the reflectivity of the telescope primary mirror and not by systematic uncertainties of the data reduction itself.

Another issue with the sensitivity function is the red-to-blue relative spectrophotometry that needs to be checked. The $g - r$ colour difference appears pretty flat with time, at least before and after the mirror coating. Apparently, the wavelength dependent reflectivity of the mirror changed slightly, which causes a systematic offset in the

colour by 0.04 ± 0.05 mag. This spectrophotometric accuracy is already better than the 10% anticipated in the design of the survey. The stability of the spectrophotometry is encouraging considering that we use an *average* sensitivity function, but we want to improve the overall accuracy even further. There are two limiting factor for the spectrophotometry: 1.The large fibers of PPAK together with the low filling factor leads to aperture losses of the standard star that are wavelength dependent due to atmospheric dispersion. 2. Changes in the wavelength-dependent atmospheric extinction curve are not monitored in real time. To overcome this limitation we plan to use a time dependent spectrophotometric and the lens array integral field unit of PMAS to obtain spectra in a $16'' \times 16''$ field for a few elliptical galaxies observed already with CALIFA. These spectra can be calibrated to much higher accuracy because of the continuous spatial coverage of the lens array and will serve as reference spectra to construct the sensitivity function from the CALIFA data itself without the aperture losses involved for pointing sources. Nevertheless, the current scheme is more than sufficient for the first 100 galaxies observed, but we anticipate that any discrepancy will increase over time and needs to be solved.

4. Error propagation and correlated noise

A significant improvement compared to the CALIFA data reduction described in Sánchez et al. (2012) is the implementation of the photon and read-out noise propagation from the raw data to the final datacube. This is possible only by reducing the number of interpolation and resampling steps to a minimum during the whole reduction process, so that the error spectra can be propagated analytically through each processing step. We only resample the individual wavelength solution of each fiber to a common wavelength grid and use a Monte Carlo scheme to propagate the error vector. The correction for DAR effects often required a resampling scheme to align the object position along the wavelength. In CALIFA we avoid this additional resampling step by a two stage process. First, we reconstruct the datacube from the individual fibers as described above and estimate the position of the galaxy centre at each wavelength. Second, we reconstruct a DAR-corrected datacube again from the individual fibers by changing the relative position of the fibers against the final grid of the datacube according to the previously estimated DAR effect. The simplicity of the spatial image reconstruction scheme allows to analytically compute the errors associated with each spectrum even in the reconstructed datacube.

However, the reconstruction of the datacube implies that the spectra and its associated noise are strongly correlated. This can be highlighted by the fact that a CALIFA datacube comprises about 4400 spectra that were constructed from a set of only 993 independent fibers. In the analysis of CALIFA datacubes it is a common task to coadd spectra together in certain bins with the aim to increase the S/N for low surface brightness regions. The spatial correlation of the noise will lead to a systematic overestimation of the formal S/N per bin, because it has been assumed that the spectra, and its associated noise, are completely independent. This effect has been empirically verified on the data as shown in Fig. 5. Although it is not feasible to handle the full co-variance matrix of a datacube, a statistical correction of the error and S/N is still possible. As part of the data reduction pipeline we compute an error weight factor needed to re-scale the formal noise of each pixel in the limit of co-adding all spectra of the datacube. We are currently studying in detail the relation of the error weight factor with bin size and

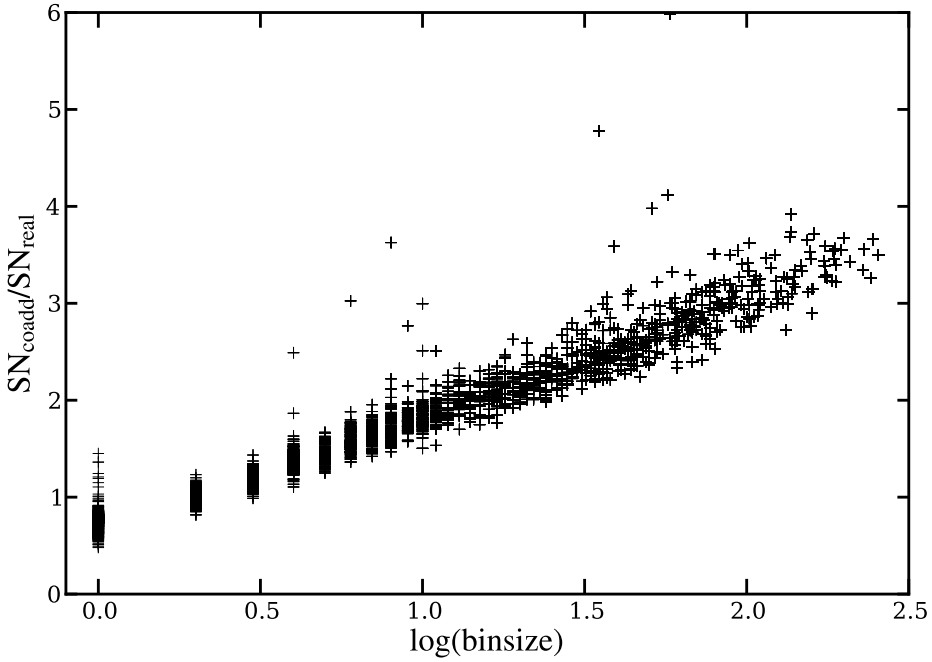

Figure 5. Signal-to-noise (SN) correction factor as a function of the number of coadded spectra within the datacube. There is a very tight relation between the formal estimated SN and the measured SN for different binsize to compute the coadded spectra. The data points originate from 15 representative datacube showing that this is a universal relation for all CALIFA datacubes considering that the same dither pattern is used for all objects. The deviations from a linear relation at low binsizes is due to contaminations of stars in the field for which the real SN was not properly estimated.

will provide a simple recipe in the DR1 article (Husemann et al. in prep.) that allows to estimate the S/N for coadd CALIFA spectra directly from the data. This will be essential to properly use the CALIFA data for almost all science applications.

5. First results and Data release

Currently, the data taken so far are being checked for their quality within the collaboration to full-fill certain figure of merits in the accuracy of the astrometry, spectrophotometry, the wavelength calibration, and other parameters that will affect the final data quality. With the aim of being a true legacy survey, the CALIFA DR1 (Husemann et al. in prep.) will release the reduced high-quality data for an initial set of 100 galaxies at the end of this year. In the meantime, the progress of the survey can be checked at http://www.caha.es/CALIFA. Subsequent data releases will follow as the survey progresses along which we are continuously working to increase the calibration and quality of data as discussed in this short article. We hope that the astronomical community as a whole will benefit from our efforts and actively use the CALIFA data for their own science projects.

Acknowledgments. This article is based on data obtained by the CALIFA Survey, funded by the Spanish Ministery of Science under grant ICTS-2009-10, and the Centro Astronómico Hispano-Alemán. Financial support for B. Husemann through the German Science Foundation (DFG) under grant Wi 1369/29-1 is gratefully acknowledged. S.F.Sánchez and D. Mast thank the *Plan Nacional de Investigación y Desarrollo* funding programs, AYA2010-22111-C03-03 and AYA2010-10904E, of the Spanish *Ministerio de Ciencia e Innovacion*, for the support given to this project. J. Falcon-Barroso acknowledges support from the *Ramón y Cajal Program* as well as grant AYA2010-21322-C03-02 by the Spanish *Ministrio de Ciencia e Innovacion*. Based on observations collected at the Centro Astronónico Hispano Alemán (CAHA) at Carla Alto, operated jointly by the Max-Planck Institut für Astronomie and the Instituto de Astrofisica de Andalucía (CSIC).

References

Cappellari, M., Emsellem, E., Krajnović, D., McDermid, R. M., Scott, N., Verdoes Kleijn, G. A., Young, L. M., Alatalo, K., Bacon, R., Blitz, L., Bois, M., Bournaud, F., Bureau, M., Davies, R. L., Davis, T. A., de Zeeuw, P. T., Duc, P.-A., Khochfar, S., Kuntschner, H., Lablanche, P.-Y., Morganti, R., Naab, T., Oosterloo, T., Sarzi, M., Serra, P., & Weijmans, A.-M. 2011, MNRAS, 413, 813. 1012.1551

Folkes, S., Ronen, S., Price, I., Lahav, O., Colless, M., Maddox, S., Deeley, K., Glazebrook, K., Bland-Hawthorn, J., Cannon, R., Cole, S., Collins, C., Couch, W., Driver, S. P., Dalton, G., Efstathiou, G., Ellis, R. S., Frenk, C. S., Kaiser, N., Lewis, I., Lumsden, S., Peacock, J., Peterson, B. A., Sutherland, W., & Taylor, K. 1999, MNRAS, 308, 459. arXiv:astro-ph/9903456

Le Fèvre, O., Vettolani, G., Paltani, S., Tresse, L., Zamorani, G., Le Brun, V., Moreau, C., Bottini, D., Maccagni, D., Picat, J. P., Scaramella, R., Scodeggio, M., Zanichelli, A., Adami, C., Arnouts, S., Bardelli, S., Bolzonella, M., Cappi, A., Charlot, S., Contini, T., Foucaud, S., Franzetti, P., Garilli, B., Gavignaud, I., Guzzo, L., Ilbert, O., Iovino, A., McCracken, H. J., Mancini, D., Marano, B., Marinoni, C., Mathez, G., Mazure, A., Meneux, B., Merighi, R., Pellò, R., Pollo, A., Pozzetti, L., Radovich, M., Zucca, E., Arnaboldi, M., Bondi, M., Bongiorno, A., Busarello, G., Ciliegi, P., Gregorini, L., Mellier, Y., Merluzzi, P., Ripepi, V., & Rizzo, D. 2004, A&A, 428, 1043. arXiv:astro-ph/0403628

Mármol-Queraltó, E., Sánchez, S. F., Marino, R. A., Mast, D., Viironen, K., Gil de Paz, A., Iglesias-Páramo, J., Rosales-Ortega, F. F., & Vilchez, J. M. 2011, A&A, 534, A8. 1106.4183

Moles, M., Benítez, N., Aguerri, J. A. L., Alfaro, E. J., Broadhurst, T., Cabrera-Caño, J., Castander, F. J., Cepa, J., Cerviño, M., Cristóbal-Hornillos, D., Fernández-Soto, A., González Delgado, R. M., Infante, L., Márquez, I., Martínez, V. J., Masegosa, J., del Olmo, A., Perea, J., Prada, F., Quintana, J. M., & Sánchez, S. F. 2008, AJ, 136, 1325. 0806.3021

Rix, H.-W., Barden, M., Beckwith, S. V. W., Bell, E. F., Borch, A., Caldwell, J. A. R., Häussler, B., Jahnke, K., Jogee, S., McIntosh, D. H., Meisenheimer, K., Peng, C. Y., Sanchez, S. F., Somerville, R. S., Wisotzki, L., & Wolf, C. 2004, ApJS, 152, 163. arXiv:astro-ph/0401427

Rosales-Ortega, F. F., Kennicutt, R. C., Sánchez, S. F., Díaz, A. I., Pasquali, A., Johnson, B. D., & Hao, C. N. 2010, MNRAS, 405, 735. 1002.1946

Roth, M. M., Kelz, A., Fechner, T., Hahn, T., Bauer, S.-M., Becker, T., Böhm, P., Christensen, L., Dionies, F., Paschke, J., Popow, E., Wolter, D., Schmoll, J., Laux, U., & Altmann, W. 2005, PASP, 117, 620. astro-ph/0502581

Sánchez, S. F. 2006, AN, 327, 850. astro-ph/0606263

Sánchez, S. F., Cardiel, N., Verheijen, M. A. W., Martín-Gordón, D., Vilchez, J. M., & Alves, J. 2007, A&A, 465, 207. arXiv:astro-ph/0611363

Sánchez, S. F., Kennicutt, R. C., Gil de Paz, A., van de Ven, G., Vílchez, J. M., Wisotzki, L., Walcher, C. J., Mast, D., Aguerri, J. A. L., Albiol-Pérez, S., Alonso-Herrero, A., Alves, J., Bakos, J., Bartáková, T., Bland-Hawthorn, J., Boselli, A., Bomans, D. J., Castillo-Morales, A., Cortijo-Ferrero, C., de Lorenzo-Cáceres, A., Del Olmo, A., Dettmar, R.-J., Díaz, A., Ellis, S., Falcón-Barroso, J., Flores, H., Gallazzi, A., García-Lorenzo, B., González Delgado, R., Gruel, N., Haines, T., Hao, C., Husemann, B., Iglésias-Páramo, J., Jahnke, K., Johnson, B., Jungwiert, B., Kalinova, V., Kehrig, C., Kupko, D., López-Sánchez, Á. R., Lyubenova, M., Marino, R. A., Mármol-Queraltó, E., Márquez, I., Masegosa, J., Meidt, S., Mendez-Abreu, J., Monreal-Ibero, A., Montijo, C., Mourão, A. M., Palacios-Navarro, G., Papaderos, P., Pasquali, A., Peletier, R., Pérez, E., Pérez, I., Quirrenbach, A., Relaño, M., Rosales-Ortega, F. F., Roth, M. M., Ruiz-Lara, T., Sánchez-Blázquez, P., Sengupta, C., Singh, R., Stanishev, V., Trager, S. C., Vazdekis, A., Viironen, K., Wild, V., Zibetti, S., & Ziegler, B. 2012, A&A, 538, A8. 1111.0962

Scoville, N., Aussel, H., Brusa, M., Capak, P., Carollo, C. M., Elvis, M., Giavalisco, M., Guzzo, L., Hasinger, G., Impey, C., Kneib, J.-P., LeFevre, O., Lilly, S. J., Mobasher, B., Renzini, A., Rich, R. M., Sanders, D. B., Schinnerer, E., Schminovich, D., Shopbell, P., Taniguchi, Y., & Tyson, N. D. 2007, ApJS, 172, 1. arXiv:astro-ph/0612305

Viironen, K., Sánchez, S. F., Marmol-Queraltó, E., Iglesias-Páramo, J., Mast, D., Marino, R. A., Cristóbal-Hornillos, D., Gil de Paz, A., van de Ven, G., Vilchez, J., & Wisotzki, L. 2012, A&A, 538, A144. 1111.5205

Wolf, C., Meisenheimer, K., Rix, H.-W., Borch, A., Dye, S., & Kleinheinrich, M. 2003, A&A, 401, 73. arXiv:astro-ph/0208345

York, D. G., Adelman, J., Anderson, J. E., Jr., Anderson, S. F., Annis, J., Bahcall, N. A., Bakken, J. A., Barkhouser, R., Bastian, S., Berman, E., Boroski, W. N., Bracker, S., Briegel, C., Briggs, J. W., Brinkmann, J., Brunner, R., Burles, S., Carey, L., Carr, M. A., Castander, F. J., Chen, B., Colestock, P. L., Connolly, A. J., Crocker, J. H., Csabai, I., Czarapata, P. C., Davis, J. E., Doi, M., Dombeck, T., Eisenstein, D., Ellman, N., Elms, B. R., Evans, M. L., Fan, X., Federwitz, G. R., Fiscelli, L., Friedman, S., Frieman, J. A., Fukugita, M., Gillespie, B., Gunn, J. E., Gurbani, V. K., de Haas, E., Haldeman, M., Harris, F. H., Hayes, J., Heckman, T. M., Hennessy, G. S., Hindsley, R. B., Holm, S., Holmgren, D. J., Huang, C., Hull, C., Husby, D., Ichikawa, S., Ichikawa, T., Ivezić, Ž., Kent, S., Kim, R. S. J., Kinney, E., Klaene, M., Kleinman, A. N., Kleinman, S., Knapp, G. R., Korienek, J., Kron, R. G., Kunszt, P. Z., Lamb, D. Q., Lee, B., Leger, R. F., Limmongkol, S., Lindenmeyer, C., Long, D. C., Loomis, C., Loveday, J., Lucinio, R., Lupton, R. H., MacKinnon, B., Mannery, E. J., Mantsch, P. M., Margon, B., McGehee, P., McKay, T. A., Meiksin, A., Merelli, A., Monet, D. G., Munn, J. A., Narayanan, V. K., Nash, T., Neilsen, E., Neswold, R., Newberg, H. J., Nichol, R. C., Nicinski, T., Nonino, M., Okada, N., Okamura, S., Ostriker, J. P., Owen, R., Pauls, A. G., Peoples, J., Peterson, R. L., Petravick, D., Pier, J. R., Pope, A., Pordes, R., Prosapio, A., Rechenmacher, R., Quinn, T. R., Richards, G. T., Richmond, M. W., Rivetta, C. H., Rockosi, C. M., Ruthmansdorfer, K., Sandford, D., Schlegel, D. J., Schneider, D. P., Sekiguchi, M., Sergey, G., Shimasaku, K., Siegmund, W. A., Smee, S., Smith, J. A., Snedden, S., Stone, R., Stoughton, C., Strauss, M. A., Stubbs, C., SubbaRao, M., Szalay, A. S., Szapudi, I., Szokoly, G. P., Thakar, A. R., Tremonti, C., Tucker, D. L., Uomoto, A., Vanden Berk, D., Vogeley, M. S., Waddell, P., Wang, S., Watanabe, M., Weinberg, D. H., Yanny, B., & Yasuda, N. 2000, AJ, 120, 1579. arXiv:astro-ph/0006396